ELECTRONIC EDGE STATES IN GRAPHENE SHEETS

OANA-ANCUTA DOBRESCU[1], M. APOSTOL[2,*]

[1]Physics Department, University of Bucharest, Magurele-Bucharest, Romania
[2]Department of Theoretical Physics, Institute of Atomic Physics,
Magurele-Bucharest, POBox MG-35, Romania
[*]corresponding author, *E-mail*: apoma@theory.nipne.ro

Received October 3, 2014

Electronic edge ("surface") states are investigated in semi-infinite graphene sheets and graphene ribbons (monolayers) with armchair, zig-zag or horseshoe edges within the nearest-neighbour tight-binding approximation. The problem is generalized to include edge elements of the hopping (transfer) matrix which are distinct from the infinite-sheet ("bulk") ones. Within this model the semi-infinite graphene sheets with zig-zag or horseshoe edges exhibit edge states, while the semi-infinite graphene sheet with armchair edge does not. The energy of the edge states derived here lies above the (zero) Fermi level. Similarly, symmetric graphene ribbons with zig-zag or horseshoe edges have edges states, while ribbons with asymmetric edges (zig-zag and horseshoe) have not. It is also shown how to construct the "reflected" solution for the intervening equations with finite differences both for semi-infinite sheets and ribbons, either with uniform matrix elements or with modified elements of the hopping matrix at the edges.

Key words: Graphene; Graphene ribbons; Electronic edge states.

PACS: 73.22.Pr; 73.20.At; 61.48.Gh; 72.80.Vp.

1. INTRODUCTION

Graphene sheets (monolayers), described as early as 1947 [1–3], have been eventually isolated and identified in 2004-2005 [4–7]. They are two-dimensional pieces of carbon (graphite) solids with honeycomb lattice (two identical inter-penetrating triangular sub-lattices). As it is well known, (free) two-dimensional solids cannot exist, because of atomic fluctuations.[8–12] In the case of graphene (as well as other two-dimensional crystals that may exist), several, more or less unknown, factors may conspire to make free-standing sheets stable, most likely their non-thermodinamic, small (finite) size (in this respect, independent, small-size graphene sheets can be viewed as instances of genuine quantum solids). Infinite, two-dimensional graphene sheets exhibit a linear spectrum of electronic excitations (Dirac massless fermions), arising from carbon π-electrons. These "bulk" states attracted much interest, especially due to their long lifetime (and mean free path), as well as their purely wavelike nature. In finite-size graphene pieces the electronic spectrum may acquire a different character. In particular, the electronic transport along well-defined

sheet edges enjoys a special attention.[13]-[24] As it is well known, the identification of the edge ("surface") states requires well-defined boundary conditions. Within the tight-binding approximation, the hopping matrix elements at the edges are modified with respect to the matrix elements of the infinite (bulk) sheet.[25]-[30] In this respect, the edge states of graphene sheets have been tackled by using the tight-binding approximation within limited assumptions (see, for instance, Ref. [21]). The usual approach assumes the same hopping matrix for the bulk and edge sites and seeks zero-energy (zero Fermi level) edge modes.[14, 15, 22, 24] In this case one sub-lattice exhibits a damped solution, while the other sub-lattice has a vanishing solution. This is a particular situation, with an identically zero tight-binding hamiltonian, the two sub-lattices being decoupled from one another. Along similar lines Klein's edge modifications[13] are considered in Ref. [22]. We show in this paper that edge states occur in graphene sheets with zig-zag or horseshoe edges within the tight-binding approximation only for modified edge hopping matrix (Tamm or Shockley surface states) and their energy lies above the (zero) Fermi level. Using the Dirac equation for identifying edge states in finite-size graphene sheets assumes massless Dirac excitations and implies the continuum limit, which is different, in general, from finite-diference equations of the tight-binding approach [31]. Wave equations admit, in general, surface states, providing suitable boundary conditions are imposed. Elementary excitations (like Dirac massless electrons in graphene) are different from electronic states; the former are small variations of electronic states (envelope wavefunctions), while the latter are obtained by imposing suitable boundary conditions. We give here an advanced description of electronic edge states in graphene sheets, by using the neareast-neighbour tight-binding approximation with generalized boundary conditions arising from edge hopping matrix which is distinct from the bulk one. As it is well known, this is an old, basic technique, employed extensively in the past in the ferromagnetism of the thin films[32–34] and derived from previous studies of electron dynamics in crystal lattices [35]. The edge states are the counterpart in two dimensions of the Tamm or Shockley surface states in three-dimensional crystals [25–27], which are derived usually in the same standard way as that employed here.

2. INFINITE SHEET

First we consider an infinite sheet of carbon hexagons as shown in Figs. 1-3. The position of an atom is identified by the vectors (m,n) and $\mathbf{v}_{1,2,3}$. For instance, the vectors $\mathbf{v}_{1,2,3}$ in Fig. 1 are given by $\mathbf{v}_1 = (1,0)$, $\mathbf{v}_2 = (-1/2, \sqrt{3}/2)$ and $\mathbf{v}_3 = (-1/2, -\sqrt{3}/2)$ (the hexagon side is taken equal to unity). It is easy to see that we get the hexagonal periodicity of the lattice by applying twice the vectors $\mathbf{v}_{1,2,3}$. The wavefunction coefficients of the tight-binding approximation (the tight-binding

amplitudes, or the annihilation operators of the on-site fermionic states) are denoted by $a^{\mathbf{v}}_{mn}$ and $b^{\mathbf{v}}_{mn}$, corresponding to the two sub-lattices, where $\mathbf{v}$ denotes one of the vectors $\mathbf{v}_{1,2,3}$, or $\mathbf{v}=0$. The equations of motion for $a^{\mathbf{v}}_{mn}$ and $b^{\mathbf{v}}_{mn}$ within the nearest-neighbour tight-binding aproximation are given by

$$\begin{aligned}
\varepsilon a_{mn} &= t(b^{\mathbf{v}_1}_{mn}+b^{\mathbf{v}_2}_{mn}+b^{\mathbf{v}_3}_{mn}),\\
\varepsilon b^{\mathbf{v}_1}_{mn} &= t^*(a_{mn}+a^{\mathbf{v}_1-\mathbf{v}_2}_{mn}+a^{\mathbf{v}_1-\mathbf{v}_3}_{mn}),\\
\varepsilon b^{\mathbf{v}_2}_{mn} &= t^*(a_{mn}+a^{\mathbf{v}_2-\mathbf{v}_1}_{mn}+a^{\mathbf{v}_2-\mathbf{v}_3}_{mn}),\\
\varepsilon b^{\mathbf{v}_3}_{mn} &= t^*(a_{mn}+a^{\mathbf{v}_3-\mathbf{v}_2}_{mn}+a^{\mathbf{v}_3-\mathbf{v}_1}_{mn}),
\end{aligned} \tag{1}$$

where ε is the energy (on-site energy included) and t is the transfer (hoping) matrix element. We get periodic solutions of this system of equations of the form

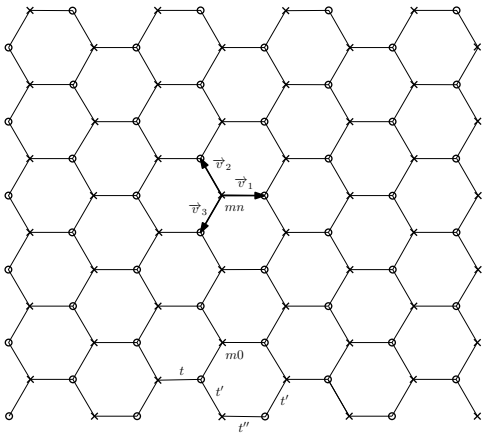

Figure 1 – Semi-infinite graphene sheet with armchair edge.

$a^{\mathbf{v}}_{mn}\sim A(\mathbf{K})e^{i\mathbf{K}[(m,n)+\mathbf{v}]}$, $b^{\mathbf{v}}_{mn}\sim B(\mathbf{K})e^{i\mathbf{K}[(m,n)+\mathbf{v}]}$, where the wavevector $\mathbf{K}$ has the components $\mathbf{K}=(k,q)$, for energies given by

$$|\lambda|^2 = 3+2\cos\mathbf{K}(\mathbf{v}_1-\mathbf{v}_2)+2\cos\mathbf{K}(\mathbf{v}_1-\mathbf{v}_3)+2\cos\mathbf{K}(\mathbf{v}_2-\mathbf{v}_3), \tag{2}$$

where $\lambda=\varepsilon/t$; making use of the vectors $\mathbf{v}_{1,2,3}$ given above, we get from equation (2)

$$|\lambda|^2=\varepsilon^2/|t|^2=1+4\cos\frac{3k}{2}\cos\frac{\sqrt{3}q}{2}+4\cos^2\frac{\sqrt{3}q}{2}. \tag{3}$$

We have also the representation

$$\lambda A=B(e^{i\mathbf{K}\mathbf{v}_1}+e^{i\mathbf{K}\mathbf{v}_2}+e^{i\mathbf{K}\mathbf{v}_3}),\quad \lambda^*B=A(e^{-i\mathbf{K}\mathbf{v}_1}+e^{-i\mathbf{K}\mathbf{v}_2}+e^{-i\mathbf{K}\mathbf{v}_3}), \tag{4}$$

which implies $A = B^*$; under these circumstances we may take t (and λ) real and equations (4) become

$$\lambda A = B(e^{ik} + 2e^{-ik/2}\cos\frac{\sqrt{3}q}{2}),\ \lambda B = A(e^{-ik} + 2e^{ik/2}\cos\frac{\sqrt{3}q}{2}). \tag{5}$$

The energy ε given by equation (3) is a well-known result;[1, 36] we can write $\varepsilon = \pm t\sqrt{S}$, where

$$S = 1 + 4\cos\frac{3k}{2}\cos\frac{\sqrt{3}q}{2} + 4\cos^2\frac{\sqrt{3}q}{2}; \tag{6}$$

the function S is positive over the Brillouin zone defined by the hexagon $3k/2 = \pm\pi$, $\sqrt{3}q/2 = \pm\pi/3$ and $k = 0$, $\sqrt{3}q/2 = \pm 2\pi/3$; it ranges from $S = 9$ at the centre of the Brillouin zone to $S = 0$ at the hexagon corners (Fermi level); at these points the energy goes like $\varepsilon = \pm(3t/2)K$, where $\mathbf{K} = (k, q)$ is the wavevector with the origin at the hexagon's corners. This is a gapless Dirac-like electronic spectrum. Graphene sheets are zero-gap semiconductors (or zero-overlap semimetals). The linear electronic spectrum is similar with the electron excitations in a normal Fermi liquid (Landau quasi-particles). Of course, the degeneracy at the gapless points in the Brillouin zone may be removed by distortions of the Jahn-Teller type, if other constraints are not present.

3. ARMCHAIR EDGE

We consider now a semi-infinite graphene sheet with armchair edge, as shown in Fig. 1. We take the site denoted by $m, 0$ as a reference site for the edge sites; the elements of the transfer matrix are modified at the edge, as shown in Fig. 1; in addition, the coefficients corresponding to the sites lying on the edge line are modified; we denote them by $a_{m0}^{'v_3-v_2}$ and $b_{m0}^{'v_1-v_2+v_3}$. The relevant equations of motion are

$$\begin{aligned}
\varepsilon b_{m0}^{\mathbf{v}_3} &= t(a_{m0} + a_{m0}^{\mathbf{v}_3-\mathbf{v}_1}) + t^{'} a_{m0}^{'\mathbf{v}_3-\mathbf{v}_2},\\
\varepsilon a_{m0}^{\mathbf{v}_1-\mathbf{v}_2} &= t(b_{m0}^{\mathbf{v}_1} + b_{m0}^{2\mathbf{v}_1-\mathbf{v}_2}) + t^{'} b_{m0}^{'\mathbf{v}_1-\mathbf{v}_2+\mathbf{v}_3},\\
\varepsilon a_{m0}^{'\mathbf{v}_3-\mathbf{v}_2} &= t^{'} b_{m0}^{\mathbf{v}_3} + t^{''} b_{m0}^{'\mathbf{v}_3-\mathbf{v}_2+\mathbf{v}_1},\\
\varepsilon b_{m0}^{'\mathbf{v}_1-\mathbf{v}_2+\mathbf{v}_3} &= t^{'} a_{m0}^{\mathbf{v}_1-\mathbf{v}_2} + t^{''} a_{m0}^{'\mathbf{v}_3-\mathbf{v}_2};
\end{aligned} \tag{7}$$

or, introducing the notations $\lambda = \varepsilon/t$, $t^{'} = t(1+\sigma)$ and $t^{''} = t(1+\rho)$,

$$\begin{aligned}
\lambda B &= A(e^{-i\mathbf{K}\mathbf{v}_3} + e^{-i\mathbf{K}\mathbf{v}_1}) + (1+\sigma)A^{'}e^{-i\mathbf{K}\mathbf{v}_2},\\
\lambda A &= B(e^{i\mathbf{K}\mathbf{v}_2} + e^{i\mathbf{K}\mathbf{v}_1}) + (1+\sigma)B^{'}e^{i\mathbf{K}\mathbf{v}_3},\\
\lambda A^{'} &= (1+\sigma)Be^{i\mathbf{K}\mathbf{v}_2} + (1+\rho)B^{'}e^{i\mathbf{K}\mathbf{v}_1},\\
\lambda B^{'} &= (1+\sigma)Ae^{-i\mathbf{K}\mathbf{v}_3} + (1+\rho)A^{'}e^{-i\mathbf{K}\mathbf{v}_1}.
\end{aligned} \tag{8}$$

We note that equations (7) or (8) correspond to generalized boundary conditions, which are richer in structure than usual boundary conditions employed for differential equations. Making use of equations (4) we get $A = (1+\sigma)A^{'}$, $B = (1+\sigma)B^{'}$ from the first two equations (8) and

$$e^{i\mathbf{K}\mathbf{v}_3} = \sigma(2+\sigma)e^{i\mathbf{K}\mathbf{v}_2} + \rho e^{i\mathbf{K}\mathbf{v}_1}, e^{-i\mathbf{K}\mathbf{v}_2} = \sigma(2+\sigma)e^{-i\mathbf{K}\mathbf{v}_3} + \rho e^{-i\mathbf{K}\mathbf{v}_1} \quad (9)$$

from the last two equations (8). We look for damped solutions of the form $\mathbf{K} = (k,q) \to (k,iq)$, corresponding to edge states $(q > 0)$; equations (9) become

$$\rho e^{i\frac{3k}{2}} + \sigma(2+\sigma)e^{-\frac{\sqrt{3}q}{2}} - e^{\frac{\sqrt{3}q}{2}} = 0, \quad (10)$$

which has no solution (except for a few isolated points in the Brillouin zone). We conclude that the semi-infinite graphene sheet with armchair edge has no edge states. Similar results are usually well-known and have been discussed recently in Ref. [24].

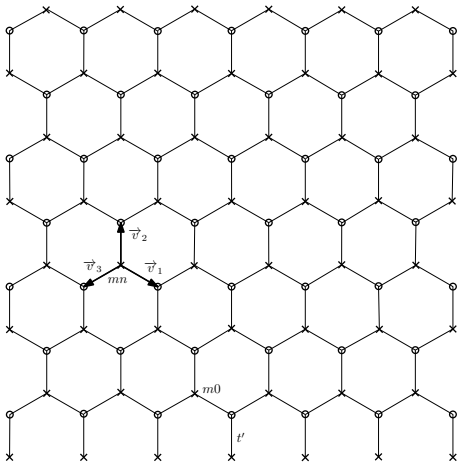

Figure 2 – Semi-infinite graphene sheet with horseshoe edge.

We note that the semi-infinite sheet has bulk states, similar with the infinite sheet. For instance, a semi-infinite sheet with a non-distorted armchair edge ($\sigma = 0$, $\rho = 0$, $A^{'} = A$, $B^{'} = B$) has the well-known "reflected" solution

$$\begin{aligned} &Ae^{i\mathbf{K}[(m,n)+\mathbf{v}]} \to A_1 e^{i\mathbf{K}[(m,n)+\mathbf{v}]} + A_2 e^{i\mathbf{K}^{'}[(m,n)+\mathbf{v}]}, \\ &Be^{i\mathbf{K}[(m,n)+\mathbf{v}]} \to B_1 e^{i\mathbf{K}[(m,n)+\mathbf{v}]} + B_2 e^{i\mathbf{K}^{'}[(m,n)+\mathbf{v}]}, \end{aligned} \quad (11)$$

where $\mathbf{K} = (k,q)$ and $\mathbf{K}^{'} = (k,-q)$. Indeed, the first two equations (8) are satisfied automatically (by virtue of equations (4)), while from the last two equations (8) we

get

$$\begin{aligned} B_1 e^{i\mathbf{K}\mathbf{v}_3} + B_2 e^{i\mathbf{K}'\mathbf{v}_3} = 0, \\ A_1 e^{-i\mathbf{K}\mathbf{v}_2} + A_2 e^{-i\mathbf{K}'\mathbf{v}_2} = 0, \end{aligned} \tag{12}$$

which gives $A_1, B_1 \sim e^{i\sqrt{3}q/2}$ and $A_2 B_2 \sim -e^{-i\sqrt{3}q/2}$. The solutions are products of plane waves along the x-direction (coordinate m) and sin-waves along the y-direction (coordinate n),

$$Ae^{i\frac{3}{2}km} \sin \frac{\sqrt{3}}{2} q(n+1), Be^{i\frac{3}{2}km} \sin \frac{\sqrt{3}}{2} q(n+1), \tag{13}$$

where we have made explicit the units and changed the origin $n = 0$ to the bottom row. We can see that the solution given by equation (13) exhibits nodes on the sites along the directions perpendicular to the edge (A and B in equation (13) are undetermined constants); it corresponds to boundary conditions $a_{mn=-1} = b_{mn=-1} = 0$. Similarly, if we set distinct hoping-matrix elements at the edge, we get reflected waves with additional constraints on the amplitudes. Such states are the well-known bulk modes.

4. ZIG-ZAG AND HORSESHOE EDGES

We discuss now two other semi-infinite graphene sheets, one with a zig-zag edge and another with a horseshoe edge, as shown in Fig. 2 and, respectively, Fig. 3. The sheet with zig-zag edge is the sheet with armchair edge rotated by the angle $-\pi/2$. The vectors $\mathbf{v}_{1,2,3}$ are given in this case by $v_1 = (\sqrt{3}/2, -1/2)$, $v_2 = (0, 1)$, $v_3 = (-\sqrt{3}/2, -1/2)$. Equations (4) for the amplitudes are preserved, while the energy is given by

$$\lambda^2 = 1 + 4\cos\frac{3q}{2}\cos\frac{\sqrt{3}k}{2} + 4\cos^2\frac{\sqrt{3}k}{2}. \tag{14}$$

(compare with equation (3)). The equations for the relevant edge sites in this case are given by

$$\begin{aligned} \varepsilon a_{m0}^{-\mathbf{v}_2} &= t b_{m0} + t' b_{m0}^{'-\mathbf{v}_2+\mathbf{v}_1} + t' b_{m0}^{'-\mathbf{v}_2+\mathbf{v}_3}, \\ \varepsilon b_{m0}^{'-\mathbf{v}_2+\mathbf{v}_1} &= t' a_{m0}^{-\mathbf{v}_2} + t' a_{m0}^{-\mathbf{v}_2+\mathbf{v}_1-\mathbf{v}_3}, \\ \varepsilon b_{m0}^{'-\mathbf{v}_2+\mathbf{v}_3} &= t' a_{m0}^{-\mathbf{v}_2} + t' a_{m0}^{-\mathbf{v}_2-\mathbf{v}_1+\mathbf{v}_3}, \end{aligned} \tag{15}$$

or

$$\begin{aligned} \lambda A &= B e^{i\mathbf{K}\mathbf{v}_2} + (1+\sigma) B' e^{i\mathbf{K}\mathbf{v}_1} + (1+\sigma) B' e^{i\mathbf{K}\mathbf{v}_3}, \\ \lambda B' &= (1+\sigma) A (e^{-iKv_1} + e^{-iKv_3}). \end{aligned} \tag{16}$$

Equations (15) admit reflected waves as bulk states, similar with equations (11); we look for edge states. Making use of equations (4) we get $B = (1+\sigma)B'$ from the first

equation (16) and

$$\sigma(2+\sigma)(e^{-i\mathbf{K}\mathbf{v}_1}++e^{-i\mathbf{K}\mathbf{v}_3})=e^{-i\mathbf{K}\mathbf{v}_2} \tag{17}$$

from the second equation (16). Equation (17) can also be written as

$$2\sigma(2+\sigma)\cos\frac{\sqrt{3}k}{2}=e^{-i\frac{3q}{2}}. \tag{18}$$

For $q\to iq$ (damped solutions along the direction perpendicular to the edge) this equation becomes

$$2\sigma(2+\sigma)\cos\frac{\sqrt{3}k}{2}=e^{\frac{3q}{2}}; \tag{19}$$

it admits solutions for $-1-\sqrt{2}/2<\sigma<-1+\sqrt{2}/2$ (except for $\sigma=-1$) or $\sigma<-1-\sqrt{6}/2$, $\sigma>-1+\sqrt{6}/2$. We conclude that the semi-infinite graphene sheet with zig-zag edge has electronic edge states, which are propagating, plane waves along the direction parallel with the edge (wavevector k) and damped waves along the direction perpendicular to the edge ($\sim e^{-q(n+v_y)}$), for values of (k,q) given by equation (19). The energy of these edge states is given by

$$\begin{aligned}\lambda^2&=1+4\cosh\frac{3q}{2}\cos\frac{\sqrt{3}k}{2}+4\cos^2\frac{\sqrt{3}k}{2}=\\&=\left[1+\frac{1}{\sigma(2+\sigma)}\right]\left[1+\frac{1}{\sigma(2+\sigma)}e^{3q}\right]=\\&=\left[1+\frac{1}{\sigma(2+\sigma)}\right]\left[1+4\sigma(2+\sigma)\cos^2\frac{\sqrt{3}k}{2}\right]\end{aligned} \tag{20}$$

for $0<q<\frac{2}{3}\ln|2\sigma(2+\sigma)|$; for each value of q there exist two values of k in the Brillouin zone which satisfy equation (19). The energy given by equation (20) lies above the (zero) Fermi level ($\lambda^2>0$). The lowest energy values ($\lambda^2\simeq 0$) correspond to the unphysical case $\sigma\simeq -1$.

It is worth noting that, according to equation (19), the edge states are absent for a uniform hoping matrix, *i.e.* for $\sigma=0$ ($t'=t$). From equation (19) the attenuation coefficient of the edge states is given by $q=\frac{2}{3}\ln[2\sigma(2+\sigma)\cos\frac{\sqrt{3}k}{2}]$, *i.e.* the wavefunction coefficients go like

$$\sim e^{ik(m+v_x)}e^{-\frac{2}{3}(n+v_y)\ln[2\sigma(2+\sigma)\cos\frac{\sqrt{3}k}{2}]}, \tag{21}$$

with amplitudes A and B related by an equation of the type (4) and $B^{'}=(1+\sigma)^{-1}B$ given above. Usually, the tight-binding approximation for edge states is applied to each sub-lattice separately for vanishing (Fermi level) energy.[14, 15, 22, 24] For instance, from the first equation (15) given above with $t^{'}=t$, $\varepsilon=0$ and $b^{'}_{m0}=b_{m0}$ we get $b_{m0}\sim -2\cos\frac{\sqrt{3}k}{2}$, $b_{mn}\sim[-2\cos\frac{\sqrt{3}k}{2}]^n=e^{n\ln[-2\cos\frac{\sqrt{3}k}{2}]}$, while $a_{mn}=0$

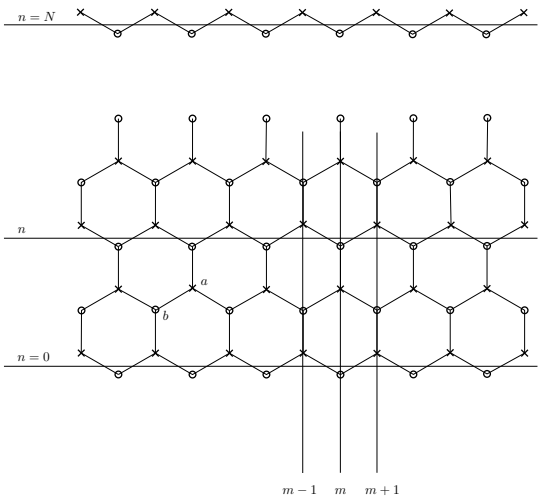

Figure 3 – Graphene ribbon with zig-zag edges.

from the last two equations (15). The same solution is obtained from equations (15) for $\varepsilon = 0$, $t^{'} \neq t$ and $B = (1+\sigma)B^{'}$. This is a particular situation, where the two sub-lattices are decoupled from one another. The boundary conditions expressed by the last two equations (15), as well as the coupling between the two sub-lattices modify appreciably the tight-binding solution, requiring in particular a different edge hoping matrix ($t^{'} \neq t$).

In order to emphasize the points discussed above it is worth investigating a semi-infinite graphene sheet with a zig-zag edge and uniform hoping-matrix elements as shown in Fig. 4. We note that the units (and the components k, q of the wavevector $\mathbf{K}$) are different from those employed before. The tight-binding equations are given by

$$\begin{aligned} &\lambda a_{mn} = b_{m+1n} + b_{m-1n} + b_{mn+1}, n = 0, 1, 2, ..., \\ &\lambda b_{mn} = a_{m+1n} + a_{m-1n} + a_{mn-1}, n = 1, 2, ..., \\ &\lambda b_{m0} = a_{m+10} + a_{m-10}. \end{aligned} \tag{22}$$

The solutions of this system of equations are of the form $a_{mn} = a_n e^{ikm}$ and $b_{mn} = b_n e^{ikm}$; the system becomes

$$\lambda a_n = 2\cos k \cdot b_n + b_{n+1}, \lambda b_n = 2\cos k \cdot a_n + a_{n-1}, n = 1, 2, ... \tag{23}$$

and

$$\lambda a_0 = 2\cos k \cdot b_0 + b_1, \lambda b_0 = 2\cos k \cdot a_0. \tag{24}$$

We set $b_n \sim r^n$ and get

$$r = x \pm \sqrt{x^2 - 1}, x = \frac{\lambda^2 - 4\cos^2 k - 1}{4\cos k} \tag{25}$$

from equations (23). We distinguish two cases. For $|x| < 1$ we may set $x = \cos q$ and get $r = e^{\pm iq}$. The solutions are of the form

$$a_n = A_1 e^{iqn} + A_2 e^{-iqn}, b_n = B_1 e^{iqn} + B_2 e^{-iqn}, \tag{26}$$

where

$$B_1 = \frac{2\cos k + e^{-iq}}{\lambda} A_1, B_2 = \frac{2\cos k + e^{iq}}{\lambda} A_2 \tag{27}$$

and

$$\lambda^2 = 4\cos^2 k + 4\cos q \cos k + 1, A_1 e^{-iq} + A_2 e^{iq} = 0; \tag{28}$$

the last condition in equations (28) corresponds to the boundary condition $a_{-1} = 0$ in equations (24). We get from the above equations

$$\begin{aligned} a_n &= 2iA_1 \sin(q(n+1), \\ b_n &= \frac{2iA_1}{\lambda} \left[2\cos k \sin q(n+1) + \sin qn\right]. \end{aligned} \tag{29}$$

These are bulk states for the semi-infinite sheet with a zig-zag edge.

For $|x| > 1$ (the second case) we may set $x = \cosh q$, $r = e^{-q}$ $(q > 0)$ and the solutions have the form $a_n = Ae^{-qn}$, $b_n = Be^{-qn}$, corresponding to edge states. From the system of equations (23) we get

$$\lambda B = (2\cos k + e^q)A \tag{30}$$

and

$$\lambda B = 2\cos k \cdot A \tag{31}$$

from the second equation (24), where $\lambda^2 = 4\cos^2 k + 4\cosh q \cos k + 1$. We can see that equations (30) and (31) have no solution. This reflects the fact that the boundary condition $a_{-1} = Ae^q = 0$ (second equation (24)) has no solution. We can attempt to satisfy equation (31) by imposing $A = 0$, which leads immediately to $\lambda = 0$, but this means that we decouple a sub-lattice. In accordance with what we have said above, the edge states appear only for non-uniform hopping-matrix elements at the edge.

We assume now that we have a different hopping-matrix element at the edge, $t^{'} = (1+\sigma)t$, and distinct amplitudes $b^{'}_{m0}$. It is easy to see that equations (22) remain the same providing we define $b^{'}_{m0}$ by $b_{m0} = (1+\sigma)b^{'}_{m0}$ and impose the boundary condition

$$(1+\sigma)^2 - 1](a_{m+10} + a_{m-10}) = a_{mn=-1}. \tag{32}$$

The bulk states are of the form given by equations (26) and (27), where $A_{1,2}$ are related through

$$[2\sigma(2+\sigma)\cos k - e^{-iq}]A_1 + [2\sigma(2+\sigma)\cos k - e^{iq}]A_2 = 0; \tag{33}$$

this equation is a generalization of the boundary condition expressed by the second equation (28). For edge states equation (30) remains valid, while equation (31)

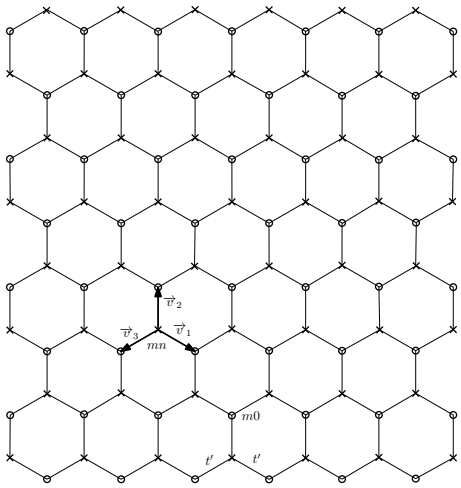

Figure 4 – Semi-infinite graphene sheet with zig-zag edge.

(boundary condition) leads to

$$2\sigma(2+\sigma)\cos k = e^q, \tag{34}$$

which is equation (19) (with different units).

Similarly, equations (4) and (14) hold for the semi-infinite sheet with a horse-shoe edge (Fig. 3) (this is a rather unrealistic situation, since the dangling bonds terminate usually with hydrogen which does not contribute to electronic states [23]. The equations for the edge sites in this case are given by

$$\begin{aligned} \varepsilon b_{m0}^{\mathbf{v}_1} &= t(a_{m0} + a_{m0}^{\mathbf{v}_1-\mathbf{v}_3}) + t' a_{m0}^{'\mathbf{v_1}-\mathbf{v}_2}, \\ \varepsilon a_{m0}^{'\mathbf{v}_1-\mathbf{v}_2} &= t' b_{m0}^{\mathbf{v}_1}. \end{aligned} \tag{35}$$

Using the same technique as for the preceding case we get the equation

$$\frac{1}{2}\sigma(2+\sigma)e^{-\frac{3q}{2}} = \cos\frac{\sqrt{3}k}{2} \tag{36}$$

for the edge states. Equation (36) has two solutions for k for each value of $q > \frac{2}{3}\ln\left|\frac{1}{2}\sigma(+\sigma)\right|$, provided $\sigma < -1-\sqrt{3}$ or $\sigma > -1+\sqrt{3}$ and for any value of $q > 0$ otherwise ($\sigma \neq 0, -1$). The energy (equation (14)) is given by

$$\begin{aligned} \lambda^2 &= 1 + 4\cosh\frac{3q}{2}\cos\frac{\sqrt{3}k}{2} + 4\cos^2\frac{\sqrt{3}k}{2} = \\ &= \left[1+\sigma(2+\sigma)\right]\left[1+\sigma(2+\sigma)e^{-3q}\right]; \end{aligned} \tag{37}$$

this energy is above the (zero) Fermi level ($\lambda^2 > 0$). Bulk states can also be obtained for this semi-infinite sheet.

5. EXTENSION TO RIBBONS

A graphene ribbon can be treated in a similar way. Let us assume such a ribbon with n-rows running from $n = 0$ to $n = N$ and with zig-zag edges. We note that a-type wavefunctions pertain to one edge, while b-type wavefunctions pertain to the other edge. The solutions consist of "reflected" waves of the form (11), which are superpositions of "direct" waves of the form $(A_1, B_1)e^{-qn}$ and "reflected" waves of the form $(A_2, B_2)e^{qn}$ (*i.e.*, $q \to iq$ in $\mathbf{K}$ and $\mathbf{K}^{'}$ in equations (11)). The desired behaviour of the reflected waves is ensured by the factor e^{-qN}, *i.e.* we set $(A_2, B_2)e^{-q(N-n)}$. The relevant equations for the N-edge are given by

$$\begin{aligned} \varepsilon b_{2mN}^{\mathbf{v}_2} &= t a_{2mN} + t^{'} a_{2mN}^{'\mathbf{v}_2-\mathbf{v}_1} + t^{'} a_{2mN}^{'\mathbf{v}_2-\mathbf{v}_3}, \\ \varepsilon a_{2mN}^{'\mathbf{v}_2-\mathbf{v}_1} &= t^{'} b_{2mN}^{\mathbf{v}_2} + t^{'} b_{2mN}^{\mathbf{v}_2-\mathbf{v}_1+\mathbf{v}_3}, \\ \varepsilon a_{2mN}^{'\mathbf{v}_2-\mathbf{v}_3} &= t^{'} b_{2mN}^{\mathbf{v}_2} + t^{'} b_{2mN}^{\mathbf{v}_2+\mathbf{v}_1-\mathbf{v}_3} \end{aligned} \tag{38}$$

(compare with equations (15)); the energy given by equation (14) remains the same, as do the equations (4) for bulk amplitudes. Equations (38) lead to the complex conjugate of equation (18), *i.e.* to the same equation (19) and the same energy for the edge states, as expected.

Making use of the notations given in Fig. 4, the tight-binding equations for a ribbon with zig-zag edges and uniform hopping-matrix elements are equations (22) with the boundary conditions $a_{mn=-1} = b_{mN+1} = 0$. Following the same procedure as for a semi-infinite sheet (equations (22) to (31)) we get the bulk states ($a_{mn} = a_n e^{ikm}$, $b_{mn} = b_n e^{ikm}$)

$$\begin{aligned} a_n &= 2iA \sin q(n+1), \\ b_n &= \frac{2iA}{\lambda}(2\cos k e^{iq} + 1)e^{iq(N+1)} \sin q(n-N-1), \end{aligned} \tag{39}$$

where λ is given by equation (28) and

$$\tan q(N+1) = -\frac{2\cos k \sin q}{2\cos k \cos q + 1}. \tag{40}$$

We can see that for finite-width ribbons there appears a constraint on the values of the wavevector (k, q), as expected. Seeking combinations of the form $(A_1, B_1)e^{-qn} + (A_2, B_2)e^{qn}$, corresponding to edge states, we arrive at equation $2\cos k \sinh q(N+2) + \sinh q(N+1) = 0$, which has no solution.

Similarly, we assume now non-uniform hopping-matrix elements for a ribbon with zig-zag edges. The tight-binding equations have the same structure as equations (22), with the boundary conditions

$$\begin{aligned} \sigma(2+\sigma)(a_{m+1n-0} + a_{m-1n-0}) &= a_{mn=-1}, \\ \sigma(2+\sigma)(b_{m+1N} + b_{m-1N}) &= b_{mN+1} \end{aligned} \tag{41}$$

and modified edge amplitudes $a^{'}_{mN}$, $b^{'}_{m0}$ given by $a_{mN} = (1+\sigma)a^{'}_{mN}$, $b_{m0} = (1+\sigma)b^{'}_{m0}$; the energy is given by $\lambda^2 = 4\cos^2 k + 4x\cos k + 1$, where $x = \cos q$ for bulk states or $x = \cosh q$ for edge states. The solutions $a_{mn} = a_n e^{ikm}$, $b_{mn} = b_n e^{ikm}$ are given by

$$\begin{aligned} a_n &= A_1 e^{iqn} + A_2 e^{-iqn}, \\ b_n &= B_1 e^{iqn} + B_2 e^{-iqn} \end{aligned} \tag{42}$$

for bulk states, with $q \to iq$ for edge states; the amplitudes $A_{1,2}$ and $B_{1,2}$ are related through

$$B_1 = \frac{2\cos k + e^{-iq}}{\lambda} A_1, \quad B_2 = \frac{2\cos k + e^{iq}}{\lambda} A_2 \tag{43}$$

and through other two equations arising from the boundary conditions (41). This way, we have a homogeneous system of four equations with four unknwons ($A_{1,2}$, $B_{1,2}$) which has non-vanishing solutions providing

$$\begin{aligned} &(2\cos k + e^{iq})[2\sigma(2+\sigma)\cos k - e^{-iq}]^2 e^{-iqN} = \\ &= (2\cos k + e^{-iq})[2\sigma(2+\sigma)\cos k - e^{iq}]^2 e^{iqN}; \end{aligned} \tag{44}$$

for edge states we replace q by iq. It is worth noting that for edge states ($q \to iq$) and large ribbon-widths ($N \gg 1$) the solutions of equation (44) are close to the solutions corresponding to the semi-infinite sheet given by equation (34). We can also notice in equation (44) that the continuum limit $q \to 0$ near (zero) Fermi level $k = \pm\frac{2\pi}{3}$ leads to

$$\frac{\sqrt{3}k \pm q}{\sqrt{3}k \mp q} = e^{-2qN}, \tag{45}$$

which is, formally, the typical condition for edge states for massless Dirac fermions in graphene.[15, 18, 19, 21] However, the electronic elementary excitations (envelope wavefunctions) are different from the electronic states. Elementary excitations are small variations of the already established electronic states, boundary conditions and edge states included.

Ribbons with armchair edges do not exhibited edge states, ribbons with horseshoe edges can be treated in likewise manner; a non-symmetric ribbon, with one zig-zag edge and the other horseshoe edge, implies two conditions of the type of equations (19) and (36) (two distinct purely imaginary wavevectors q), which restrict appreciably the edge states. Bulk states with restricted particular values of the wavevectors $\mathbf{K}$ may exist in ribbons, beside edge states. In general, modified hopping matrix elements at edges complicate to a great extent the boundary conditions for finite-difference equations in comparison with the differential equations of the continuum limit, pointing toward a richer structure of the physical states.

6. CONCLUSION

The tight-binding approximation has been employed here to describe the electronic edge states of semi-infinite sheets of graphene with various edge shapes (armchair, zig-zag, horseshoe). The treatment has been extended to finite-width graphene ribbons and, in addition, bulk states, which imply reflected waves, have been discussed. The main point of the treatment presented here consists in extending the dynamics of electrons in graphene to realistic situations where the hopping (transfer) matrix at the edges is different from the bulk one. Specifically, it has been shown here that the edge states exist only for distinct edge hopping matrix, corresponding to the well-known Tamm and Shockley surface states in three-dimensional solids. It has been pointed out that the edge modifications associated with finite-size graphene sheets (and finite-size solids in general), expressed in distinct edge hopping-matrix elements within the tight-binding approximation, can be viewed as a generalization of the usual boundary conditions employed currently in the continuum-limit differential equations (Dirac equation included in the case of graphene), which may lead to a richer structure of the physical states. It has also been shown that the usual tight-binding treatment of the edge electronic states in finite graphene sheets is based on limited assumptions, focussing on zero-energy (Fermi level) states which leaves aside the mutual coupling of the two graphene-sheet sub-lattices.

In conclusion we may say that semi-infinite graphene sheets with zig-zag or horseshoe edges exhibit electronic edge states within the nearest-neighbour tight-binding approximation, as do the ribbons with these same (symmetric) edges, while the semi-infinite graphene sheet with armchair edge does not, within the same approximation. Similar results have been reported before within special, limited assumptions regarding zero-energy states, uniform elements of the hoping matrix and decoupled sub-lattices. We have assumed here an infinite length along one axis (x-axis); this condition can be removed, by considering a finite length along this axis too, as for a rectangular piece of graphene sheet. The tight-binding treatment can be conducted in this case along the same lines as described above. Another interesting generalization relates to a graphene finite-size bi- or multi-layer. The main point discussed here was the generalization of the tight-binding approximation to an edge hopping matrix distinct from the bulk one, which allows the description of edge states with a non-vanishing energy (above the Fermi level).

Acknowledgements. The authors are indebted to the members of the Seminar of Theoretical Physics at Magurele-Bucharest for fruitful discussions, and to their coleague G. Vaman for bringing this problem to their attention. Collaborative atmosphere of the Institute for Physics and Nuclear Engineering at Magurele-Bucharest is also gratefully acknowledged. This work has been supported by Grants #09370102/2009 and #116/2011 of the Romanian Governmental Agency of Scientfic Research.

REFERENCES

1. P. R. Wallace, "The band theory of graphite", Phys. Rev. **71** 622-634 (1947).
2. J. W. McClure, "Diamagnetism of graphite", Phys. Rev. **104** 666-671 (1956).
3. J. C. Slonczewski and P. R. Weiss, "Band structure of graphite", Phys. Rev. **109** 272-279 (1958).
4. K. S. Novoselov, A. K. Geim, S. V. Morozov, D. Jiang, Y. Zhang, S. V. Dubonos, I. V. Grigorieva and A. A. Firsov, "Electric field effect in atomically thin carbon films", Science **306** 666-669 (2004).
5. K. S. Novoselov, D. Jiang, F. Schedin, T. J. Booth, V. V. Khotkevich, S, V. Morozov and A. K. Geim, "Two dimensional atomic crystals", Proc. Natl. Acad. Sci. USA **102** 10451-10453 (2005).
6. K. S. Novoselov, A. K. Geim, S. V. Morozov, D. Jiang, M. I. Katsnelson, I. V. Grigorieva , S. V. Dubonos and A. A. Firsov, "Two dimensional gas of massless Dirac fermions in graphene", Nature **438** 197-200 (2005).
7. Y. Zhang, J. W. Tan, H. L. Stormer and P. Kim, "Experimental observation and the quantum Hall effect and Berry's phase in graphene", Nature **438** 201-204 (2005).
8. R. Peierls, "Remarks on transition temperatures", Helv Phys. Acta **7**, Suppl. 2, 81-83 (1934).
9. L. Landau, "Theory of phase transformations. II", ZhETF **7** 627-632 (1937) (Phys. Z. Sowjetunion, "Zur Theorie der Phasenumwandlungen", **11** 545-549 (1938)).
10. L. Landau and E. Lifshitz, *Course of Theoretical Physics*, vol 5, *Statistical Physics*, Part I, Pergamon, Oxford (1980).
11. N. N. Mermin, "Crystalline order in two dimensions", Phys. Rev. **176** 250-254 (1968).
12. M. Apostol, "On the low dimensional solids and their melting", Synthetic Metals **79** 253-257 (1996).
13. D. J. Klein, "Graphitic polymer strips with edge states", Chem. Phys. Lett **217** 261-265 (1994).
14. M. Fujita, K. Wakabayashi, K. Nakada and K. Kusakabe, "Peculiar localized states at zigzag graphite edge", J. Phys. Soc. Jpn. **65** 1920-1923 (1996).
15. K. Nakada, M. Fujita, G. Dresselhaus and M. S. Dresselhaus, "Edge states in graphene ribbons: nanometer size effects and edge shape dependence", Phys. Rev. **B54** 17954-17961 ((1996).
16. K. Wakayabashi, M. Fujita, H. Ajiki and M. Sigrist, "Electronic and magnetic properties of nanographite ribbons", Phys. Rev. **B59** 8271-8282 (1999).
17. K. Wakayabashi and M. Sigrist, "Zero-conductance resonances due to flux states in nanographite ribbons", Phys. Rev. Lett. **84** 3390-3393 (2000).
18. L. Brey and H. Fertig, "Edge states and the quantized Hall effect in graphene", Phys. Rev. **B73** 195408 (2006) (1-5).
19. L. Brey and H. Fertig, "Electronic states of graphene nanoribbons studied with the Dirac equation", Phys. Rev. **B73** 235411 (2006) (1-5).
20. L. Yang, C.-H. Park, Y.-W. Son, M. L. Cohen and S. G. Louie, "Quasiparticle energies and band gaps in graphene nanoribbons", Phys. Rev. Lett. **99** 186801 (2007) (1-4).
21. A. H. Castro Neto, F. Guinea, N. M. R. Peres, K. S. Novoselov and A. K. Geim, "The electronic properties of graphene", Revs. Mod. Phys. **81** 109-162 (2009).
22. K. Wakabayashi, S. Okada, R. Tomita, S. Fujimoto and Y. Natsume, "Edge states and flat bands of graphene nanoribbons with edge modification", J. Phys. Soc. Jpn. **79** 034706 (2010) (1-7).
23. K. W. Lee and and C. E. Lee, "Edge states in horseshoe-shape carbon nanotubes transformed by hydrogen adsorption", Phys. Rev. **B87** 235119 (2013) (1-4).
24. N.T. Cuong, M. Otani and S. Okada, "Absence of edge states near the 120° corners of zig-zag graphene nanoribbons", Phys. Rev. **B87** 045424 (2013) (1-5).
25. I. Tamm, "Uber eine mogliche Art der Elektronenbindung an Krystalloberflachen", Z. Phys. **76**

849-850 (1932).
26. I. Tamm, "On the posssible bound states of electrons on a crystal surface", Phys. Z. Sowjet. **1** 733-746 (1932).
27. W. Shockley, "On the surface states associated with a periodic potential", Phys. Rev. **56** 317-323 (1939).
28. M. Ezawa, "Peculiar width dependence of the electronic properties of carbon nanoribbons", Phys. Rev. **B73** 045432 (2006) (1-8).
29. T. Kawai, Y. Miyamoto, O. Sugino and Y. Koga, "Graphitic ribbons without hydrogen termination: electronic structures and stabilities", Phys. Rev. **B62** R16349-R16352 (2000).
30. Y.-W. Son, M. L. Cohen and S. O. Louie, "Energy gaps in graphene nanoribbons", Phys. Rev. Lett. **97** 216803 (1-4).
31. A. R. Akhmerov and C. W. J. Beenakker, "Boundary conditions for Dirac fermions on a terminated honeycomb lattice", Phys. Rev. **B77** 085423 (2008) (1-10).
32. A. Corciovei, "Spin-Wave theory of thin ferromagnetic films", Phys. Rev. **130** 2223-2229 (1963).
33. A. Corciovei, G. Costache and D. Vamanu, "Ferromagnetic thin films", in Solid State Physics, eds. H. Ehrenreich, F. Seitz and D. Turnbull, **27** 237-350 (1972).
34. A. Corciovei, "On the "cyclic condition" in the study of the secular problem for finite one dimensional bodies", Rev. Roum. Phys. **10** 3-13 (1965).
35. L. Brillouin and M. Parodi, "Propagation des ondes dans les millieux periodiques", Mason, Dunod, Paris (1956).
36. B. Partoens and F. M. Peeters, "From graphene to graphite: electronic structure around the K point", Phys. Rev. **B74** 075404 (2006).